# Ca²⁺-Dependent Enhancement of Release by Subthreshold Somatic Depolarization

**Jason M. Christie**[1], **Delia N. Chiu**[1,2], and **Craig E. Jahr**[1]

[1] Vollum Institute, Oregon Health & Science University, Portland, OR USA

[2] Neuroscience Graduate Program, Oregon Health & Science University, Portland, OR USA

## Summary

In many neurons, subthreshold somatic depolarization can spread electrotonically into the axon and modulate subsequent spike-evoked transmission. Although release probability is regulated by intracellular $Ca^{2+}$, the $Ca^{2+}$-dependence of this modulatory mechanism has been debated. Using paired recordings from synaptically connected molecular-layer interneurons (MLIs) of the rat cerebellum, we observed $Ca^{2+}$-mediated strengthening of release following brief subthreshold depolarization of the soma. Two-photon microscopy revealed that, at the axon, somatic depolarization evoked $Ca^{2+}$ influx through voltage-sensitive $Ca^{2+}$ channels (VSCCs) and facilitated spike-evoked $Ca^{2+}$ entry. Exogenous $Ca^{2+}$ buffering diminished these $Ca^{2+}$ transients and eliminated the strengthening of release. Axonal $Ca^{2+}$ entry elicited by subthreshold somatic depolarization also triggered asynchronous transmission that may deplete vesicle availability and thereby temper release strengthening. In this cerebellar circuit, activity-dependent presynaptic plasticity depends on $Ca^{2+}$ elevations resulting from both sub- and suprathreshold electrical activity initiated at the soma.

Short-term alteration in the strength of neurotransmission can result from the electrotonic spread of subthreshold depolarization from the soma to presynaptic sites of release on the axon[1–3]. Mechanisms that trigger or modulate neurotransmission are often mediated through control of VSCCs because the likelihood of vesicle fusion is largely determined by the intracellular $[Ca^{2+}]$. Although high concentration $Ca^{2+}$ elevations are required to rapidly trigger exocytosis[4,5], low concentration elevations can augment subsequent release via vesicle recruitment, priming, and sensitization[6]. Because of their large amplitude, action potentials are efficient triggers for VSCC activation[7–10] and release. However, direct recordings from calyceal nerve terminals show that even slight depolarization can open VSCCs, albeit at low probability, and strengthen subsequent spike-evoked neurotransmission[11,12]. In contrast, in dentate granule cells of the hippocampus, short-term strengthening of release elicited by modest somatic depolarization may be $Ca^{2+}$-

Address for Correspondence: Jason M. Christie, Max Planck Florida Institute, 5353 Parkside Drive, Jupiter, FL 33458, Phone: (561) 799-8300, Fax: (561) 799-8374, jason.christie@maxplanckflorida.org.

independent[1,13]. Whether somatic depolarization enhances action potential-evoked release by activating axonal VSCCs in inhibitory neurons has not been addressed, although asynchronous release is augmented in a $Ca^{2+}$-dependent manner in young animals[14].

MLIs of the cerebellum, including stellate and basket cells, make inhibitory GABAergic synapses onto Purkinje cells as well as other MLIs[15]. Depolarizing potentials originating in the somatodendritic compartment of MLIs passively propagate into their axonal arbor[16,17] and open VSCCs[18]. However, action potentials are required to rapidly coordinate release from presynaptic sites, thereby limiting the voltage range for VSCC activation to subthreshold depolarization. Whether axonal $Ca^{2+}$ entry evoked by subthreshold somatic depolarization is sufficient to alter spike-evoked neurotransmission has not been directly determined in MLIs.

Here, we investigated the mechanisms that mediate somatic voltage control of axonal transmitter release between MLIs using paired electrical recording and two-photon laser scanning microscopy (2PLSM). Subthreshold somatic depolarization was sufficient to activate axonal VSCCs, elicit $Ca^{2+}$ influx and strengthen both action potential-evoked and asynchronous transmitter release. Enhancement of release was diminished or eliminated by chelating intracellular $Ca^{2+}$ with EGTA or by blocking VSCCs, indicating that there is a direct connection between somatic voltage-control of neurotransmission and $Ca^{2+}$ entry at the site of release. This suggests that release plasticity elicited by subthreshold somatic depolarization depends on presynaptic VSCCs.

## Results

### Subthreshold depolarization enhances AP-evoked release

GABA$_A$ receptor (GABA$_A$R)-mediated synaptic transmission was examined between pairs of MLIs in rat cerebellar slices using simultaneous whole-cell recording. Action potentials elicited in presynaptic cells by somatic current injection (100 – 600 pA, 3 – 5 ms) evoked time-locked inward currents in voltage-clamped postsynaptic cells ($E_{Cl^-} \approx 0$ mV) that were blocked by picrotoxin (100μM; $3.8 \pm 1.8$ % of control; n = 5). Irreversible rundown of evoked transmission, commonly observed in paired MLI recordings[19], was eliminated by presynaptic perforated patch recording[20] (see Methods). To determine whether somatic depolarization was sufficient to alter the strength of neurotransmission, presynaptic neurons were briefly depolarized from rest ($-73.3 \pm 0.3$ mV; n = 40) to a potential just subthreshold for spiking ($-56.1 \pm 0.9$ mV, 300 ms). This depolarization was followed by action potential stimulation (10 ms delay). IPSCs evoked by action potentials preceded by subthreshold depolarization were larger than interleaved control IPSCs evoked by action potentials alone ($121.1 \pm 4.8\%$ of control amplitude; n = 40, $P < 0.001$; Fig. 1a). Furthermore, the paired-pulse ratio (PPR = IPSC$_2$/IPSC$_1$) of IPSCs evoked by two action potentials (250 ms interval; PPR = $1.000 \pm 0.064$, n = 37; Fig. 1a, 1b) following subthreshold depolarization was significantly reduced compared to non-depolarized control trials ($P = 0.002$; Fig. 1b, 1c). This indicates that subthreshold somatic depolarization causes a short-term alteration in presynaptic release resulting from the electrotonic spread of the somatic depolarization into the axon, as observed in other neurons[1–3,13].

Control recordings included both facilitating and depressing responses (Fig. 1c), indicating that synapses between MLIs with different release probabilities co-exist in cerebellum. Synaptic strengthening caused by subthreshold depolarization depended on basal release probability, as the amount of enhancement of $IPSC_1$ was correlated with the PPR measured in control trials (Fig. 1d). Depressing synapses, on average, were not altered by subthreshold depolarization ($P = 0.17$). However, there was considerable variability within this group, with some pairs showing release enhancement while others were weakened (Fig. 1e). In 3 mM extracellular $Ca^{2+}$ release enhancement caused by subthreshold depolarization was less than in 1.5 mM $Ca^{2+}$ (Fig. 1e), but the increase was still significant ($P = 0.03$). High extracellular $Ca^{2+}$ increased release probability, as reflected by larger control IPSCs (peak amplitude $306.0 \pm 67.0$ and $172.7 \pm 22.5$ pA, 3.0 and 1.5 mM $Ca^{2+}$, respectively, n = 13 and 40, $P = 0.02$) and paired-pulse depression in all recordings (n = 11, Fig. 1f). Thus, strengthening of release by subthreshold depolarization is similar to other activity-dependent forms of release enhancement, such as spike-evoked facilitation and augmentation, in that these processes occur more readily in low release probability synapses.

### Subthreshold depolarization and presynaptic $Ca^{2+}$ entry

Intracellular $Ca^{2+}$ is known to govern many aspects of transmitter release6. Therefore, we probed for presynaptic $Ca^{2+}$ elevation evoked by subthreshold somatic depolarization using 2PLSM. MLIs were filled through the whole-cell patch pipette with Alexa Fluor 594 to visualize cell morphology and the $Ca^{2+}$ indicator Fluo-5F to detect intracellular $Ca^{2+}$ transients (Fig. 2a). Axon varicosities were targeted for optical recording. These varicosities are known to be hotspots of action potential-evoked $Ca^{2+}$ entry and, therefore, are presumed to be *en passant* sites of release15,18,21,22, though it remains possible that these specializations may include non-synaptic sites.

In current-clamped MLIs, subthreshold somatic depolarization (300 ms) often evoked small $Ca^{2+}$ transients in axon varicosities (Fig. 2b; Sub $Ca^{2+}$). The amplitude of these $Ca^{2+}$ transients varied across recording sites, including many varicosities without any apparent $Ca^{2+}$ elevation (Fig. 2c). However, on average, $Ca^{2+}$ responses were significantly larger than corresponding measurements obtained from interleaved control trials without subthreshold depolarization ($\Delta$ G/R $-0.0010 \pm 0.0004$ and $0.0026 \pm 0.0010$, control and depolarized, respectively; $P < 0.0001$; n = 35). In addition, we observed that $Ca^{2+}$ transients evoked by action potentials following subthreshold depolarization were larger than those without prior depolarization (Fig. 2b). Subtraction of the $Ca^{2+}$ elevation evoked during the subthreshold depolarization revealed that the facilitation of spike-evoked $Ca^{2+}$ ($24.5 \pm 4.5\%$ increase in peak amplitude, $P < 0.001$) was not merely the result of the shift in baseline fluorescence, but rather a true enhancement of spike-induced $Ca^{2+}$ influx (Fig. 2b; AP $Ca^{2+}$). The amount of spike-evoked $Ca^{2+}$ facilitation was not correlated with the amplitude of $Ca^{2+}$ influx during subthreshold depolarization (Fig. 2c). Whether this indicates that the two components contributing to $Ca^{2+}$ elevation are not causally related is unclear because the extremely small amplitude of the subthreshold response interferes with our ability to accurately measure it. However, in 3 mM extracellular $Ca^{2+}$, the $Ca^{2+}$ transient resulting from subthreshold depolarization was larger than that in control conditions (Peak $\Delta$ G/R $0.0036 \pm 0.0008$ and $0.0061 \pm 0.0030$; 1.5 and 3.0 extracellular $Ca^{2+}$, respectively; n = 35 and 74, $P =$

0.04) and was correlated with the facilitation of the spike-induced $Ca^{2+}$ influx ($r^2 = 0.19$; $P = 0.0002$), suggesting that the $Ca^{2+}$ elevation during subthreshold depolarization caused the spike-induced facilitation.

Inhibition of VSCCs by a combination of antagonists (ω-conotoxin MVIIC 1μM, SNX 0.3 μM, nimodipine 20 μM, and mibefradil 10μM) confirmed that subthreshold depolarization-evoked $Ca^{2+}$ entry occurs through VSCCs (Supplemental Fig. 1a, 1b) as previously reported[18]. The unblocked component presumably reflects toxin-resistant VSCCs[22–24], as spike-evoked $Ca^{2+}$ transients were blocked to a similar extent (Supplemental Fig. 1b). Subthreshold depolarization-induced facilitation of spike-evoked $Ca^{2+}$ entry was also diminished by VSCC inhibition ($8.7 \pm 5.0\%$ of control; n = 9, $P = 0.002$), again suggesting that this facilitation was dependent on an increase in intracellular $Ca^{2+}$ elicited by the preceding subthreshold depolarization.

Release strengthening caused by subthreshold depolarization in MNTB calyceal nerve terminals is inhibited by $Ca^{2+}$chelation, implying an alteration in an underlying $Ca^{2+}$ elevation[11,12]. In MLI axonal varicosities, depolarization-evoked $Ca^{2+}$ entry was not significantly altered by the cell-permeable $Ca^{2+}$ buffer EGTA-AM (10–20 μM; >10 min; $P = 0.08$, Fig. 3a, 3b). However, in many cases subthreshold depolarization did not result in a measurable $Ca^{2+}$ transient (see Fig. 2c) and, therefore, an effect of chelation overall could only be determined indirectly, using paired recording (see below). To test for a direct effect of chelation on $Ca^{2+}$ elevation induced by subthreshold depolarization, we focused our analysis on large-amplitude responses ( G/R > 0.0050; n = 4; Fig. 3a). In this group, EGTA significantly reduced the $Ca^{2+}$ transients ( G/R 0.0090 ± 0.0019 and 0.0043 ± 0.0027, control and EGTA, respectively, n = 4, $P = 0.03$). Facilitation of spike-evoked $Ca^{2+}$ entry following subthreshold depolarization was greatly diminished by EGTA across all cells (Fig. 3c), indicating that, even in cases where depolarization did not produce a measurable increase in $Ca^{2+}$, facilitation of the spike-evoked $Ca^{2+}$ transient was $Ca^{2+}$-dependent[25,26]. EGTA also reduced $Ca^{2+}$ transients evoked by single action potentials alone (70.1 ± 3.3% of control; n = 9, $P = 0.008$; Fig. 3a), suggesting a competition between Fluo-5F and EGTA for $Ca^{2+}$ binding[27], that basal $Ca^{2+}$ levels are sufficient to partially facilitate VSCC opening, or that there was a substantial rundown of VSCC opening.

## Enhancement of release is $Ca^{2+}$-dependent

In paired MLI recordings, the enhancement of $IPSC_1$ by subthreshold depolarization was blocked by EGTA-AM (20 μM; >10 min; 122.2 ± 7.4 and 97.5 ± 6.9% of control amplitude, −EGTA and +EGTA, respectively, n = 9, $P = 0.009$; Fig. 4a, 4b). This indicates that the increase in spike-evoked release caused by subthreshold depolarization depends on the EGTA-sensitive $Ca^{2+}$ elevation observed in axon varicosities. The block of release-strengthening by EGTA occurred mainly in recordings showing paired-pulse facilitation in control conditions. On average, IPSCs in depressing cell pairs were unaltered by subthreshold depolarization and remained unchanged with the addition of EGTA (Fig. 4b, top; see also Fig. 1e). It follows that the magnitude of the EGTA effect was correlated with the control PPR (Fig. 4b, bottom). This reinforces the conclusion that subthreshold

depolarization differentially affects release at MLI synapses in a release probability-dependent manner.

EGTA did not affect the amplitude of IPSCs evoked without preceding subthreshold depolarization (Fig. 4c; IPSC amplitudes $97.5 \pm 4.8$ and $82.8 \pm 11.3\%$ of control; n = 5 and 4, $P$ = 0.47 and 0.16; facilitating, and depressing responses, respectively). This implies that the $Ca^{2+}$ domain responsible for triggering exocytosis is tightly associated with release-competent vesicles[28,29]. However, EGTA altered the PPR, changing facilitation to depression, though it had no clear effect on depressing cell pairs (Fig. 4c, 4d; PPR for depressing cells $0.67 \pm 0.09$ and $0.97 \pm 0.09$, control and EGTA, respectively; n = 4, $P$ = 0.13). This suggests that, in basal conditions, residual $Ca^{2+}$ following an initial spike facilitates subsequent release[27] and may mask depression[30,31]. EGTA did not induce a significant change in the PPR in these responses when subthreshold depolarization preceded spiking (PPR $0.79 \pm 0.05$ and $1.01 \pm 0.11$ EGTA and +EGTA, respectively; n = 5, $P$ = 0.18), suggesting little additional or underlying modification of release in this condition.

### Subthreshold depolarization and asynchronous release

At some synapses, asynchronous release can result from the low concentration of $Ca^{2+}$ remaining after spike firing[32,33]. In our paired recordings, there was often a small increase in the frequency of asynchronous IPSCs during subthreshold somatic depolarization (Fig. 5a) likely caused by the elevation of $Ca^{2+}$ by the depolarizing stimulus. Although in many recordings, spike-evoked IPSCs from unclamped surrounding MLIs likely overwhelmed this small increase in asynchronous transmission, charge integration of averaged postsynaptic currents revealed a difference between control and depolarized trials across cells (Fig. 5b). The increase of asynchronous IPSCs by presynaptic somatic depolarization was much clearer when background action potential-driven release from spontaneously firing surrounding cells was blocked with TTX (1 μM) and the stimulus duration was prolonged (150 s; 3 mM extracellular $Ca^{2+}$; Fig. 6a, 6b, and 6d). Block of VSCCs by $Cd^{2+}$ and $Ni^{2+}$ (100 μM) eliminated depolarization-evoked asynchronous release without affecting basal spontaneous transmission (Fig. 6c, 6e), demonstrating the connection between somatic depolarization, axonal VSCC activation, and asynchronous release.

Asynchronous release elicited by repetitive firing weakens subsequent action potential-evoked phasic transmission by depleting the pool of readily-releasable vesicles[33,34]. Vesicle availability may, in part, regulate release strengthening induced by subthreshold depolarization. To explore this idea, we reduced the releasable pool of vesicles with a train of presynaptic action potentials (10 spikes, 60 Hz) and then tested for subthreshold depolarization-induced enhancement of release (Fig. 7a). The amplitude of spike-evoked test IPSCs following burst firing was reduced compared to interleaved trials without the burst ($77.3 \pm 7.0\%$ of control; n = 10, $P$ = 0.05, Fig. 7b), a result consistent with depression induced by vesicle depletion. In addition, burst firing eliminated release-strengthening elicited by subthreshold depolarization (Fig. 7a, 7c). This indicates that in conditions that diminish the releasable pool of vesicles, subthreshold depolarization is less effective in altering release probability. By extension, asynchronous release elicited by subthreshold depolarization likely limits the strengthening of spike-evoked transmission by depleting the

readily-releasable pool of vesicles. This may explain why in some cell pairs (4 of 10) the additive effect of subthreshold depolarization and bursting resulted in a weakening of transmission rather than enhancement (Fig. 7a, 7c).

## Discussion

We report that subthreshold somatic depolarization passively spreads into the axon arbor of MLIs and strengthens subsequent action potential-evoked release of GABA onto neighboring cells. Therefore, subthreshold depolarization enhancement of release is not limited to excitatory neurons, but also includes inhibitory neurons as well. We show that for MLIs, this enhancement of release depends on the opening of VSCCs, which results in $Ca^{2+}$ elevation as well as facilitation of spike-evoked $Ca^{2+}$ influx, a novel finding. An increase in asynchronous release that accompanies the subthreshold depolarization is $Ca^{2+}$-dependent and may decrease the capacity for release strengthening owing to vesicle depletion. Our results suggests the possibility that subthreshold potentials may modify neurotransmission at synapses throughout the nervous system in a $Ca^{2+}$-dependent manner, as do other forms of short-term facilitation.

### Somatic depolarization and $Ca^{2+}$ influx at sites of release

Axons are not electrotonically isolated from the somatodendritic compartment, but rather support the electrotonic spread of subthreshold somatodendritic potentials[1–3,16,18]. As a result, the open probability of voltage-sensitive ion channels in axons can be modified by somatodendritic depolarization. Our $Ca^{2+}$ measurements indicate that somatic depolarizations electrotonically spread into MLI axons and are sufficient to open VSCCs. Though not directly determined in this report, axonal length constants can exceed 400 μm in some neurons[1–3,35]. This parameter must be convolved with the number and composition of VSCCs at sites of release to determine subthreshold depolarization-mediated $Ca^{2+}$ entry[36]. In calyceal terminals, P/Q-type VSCCs open at low probability following slight depolarization[11] ($<-60$ mV), an activation range below that previously reported[25,37]. Although MLI varicosities express P/Q/N-type channels, among others[22], the VSCC subtypes mediating depolarization-evoked $Ca^{2+}$ influx remain unclear. It is possible that low-activation threshold VSCCs, such as R-type channels, preferentially mediate this $Ca^{2+}$ influx, as predicted for hippocampal mossy fiber boutons[36]. It is unknown whether $Ca^{2+}$-induced $Ca^{2+}$ release from intracellular stores[38] contributes to subthreshold depolarization-evoked $Ca^{2+}$ transients.

Subthreshold depolarization not only induces direct influx of $Ca^{2+}$ in MLI axons but also facilitates action potential-evoked $Ca^{2+}$ entry. This effect is probably dependent on the preceding influx of $Ca^{2+}$, because both inhibition of VSCCs and $Ca^{2+}$ chelation diminished the facilitation of spike-evoked $Ca^{2+}$ entry. At some synapses, VSCC-mediated currents are enhanced following $Ca^{2+}$ binding by neuronal calcium sensor 1 (NCS-1), which induces shortening of the activation phase of VSCCs[26,39]. VSCC facilitation is elicited by both supra- and subthreshold depolarization-evoked $Ca^{2+}$ elevation and is mitigated by exogenous $Ca^{2+}$ buffering[12,25,26]. In MLIs, enhancement of spike-evoked $Ca^{2+}$ entry following subthreshold depolarization could reflect a comparable $Ca^{2+}$-dependent

facilitation of VSCC activity, as MLIs express NCS-1 at presynaptic sites of release[40,41]. It remains possible that facilitation of action potential-evoked $Ca^{2+}$ entry does not depend directly on the $Ca^{2+}$ elevation evoked by the subthreshold depolarization. Alternatively, because spike-evoked $Ca^{2+}$ influx in presynaptic terminals is, in part, controlled by the amplitude and duration of the action potential waveform[9,42], facilitation of spike-evoked $Ca^{2+}$ entry following subthreshold depolarization may reflect an alteration of the underlying action potential. Prolonged subthreshold somatic depolarization inactivates axonal Kv1 potassium channels in L5 pyramidal cells of visual cortex, leading to spike broadening[3], which should in turn enhance $Ca^{2+}$ entry[42]. However, potassium channel inactivation is not expected to be EGTA-sensitive or depend on VSCCs, arguing against this possibility.

### Somatic depolarization and enhancement of release

Presynaptic receptor-mediated depolarization of calyceal nerve terminals elicits VSCC $Ca^{2+}$ elevation and strengthening of release[11,43]. Our results extend this finding; subthreshold excitatory potentials need not only be elicited on or near terminals to enhance release. Depolarizing potentials evoked in the dendrites or soma spread through the axon, opening VSCCs, elevating $Ca^{2+}$ at presynaptic specializations, and thereby increasing the likelihood of transmission. Small $Ca^{2+}$ transients increase the probability of fusion by increasing microdomain $Ca^{2+}$[44,45], recruiting or sensitizing vesicles through $Ca^{2+}$ binding by a high-affinity sensor distinct from the exocytosis trigger[27,46], and saturating endogenous $Ca^{2+}$ buffers[44,45]. If these mechanisms are mediated by residual $Ca^{2+}$ following action potential firing, then they may also be triggered by $Ca^{2+}$ influx during subthreshold depolarization[12]. Given that release probability is steeply dependent on the intracellular $[Ca^{2+}]$[4,5], enhancement of spike-evoked $Ca^{2+}$ entry will also strengthen transmission[12,25,26,42] unless the release process is saturated. If this occurs in MLIs, it may explain why high release probability synapses have a diminished capacity for release-strengthening induced by subthreshold depolarization.

We show that axonal VSCC-mediated $Ca^{2+}$ entry elicited during presynaptic depolarization is sufficient to evoke asynchronous release in MLIs. $Ca^{2+}$-induced asynchronous fusion has a relatively high sensitivity to intracellular $[Ca^{2+}]$, with an elevation to as little as 1 μM triggering release[4,5]. If the $Ca^{2+}$ sensor for asynchronous exocytosis at MLIs has a similar sensitivity, then the intracellular $[Ca^{2+}]$ reached at MLI varicosities may be much higher than depolarization-evoked $Ca^{2+}$ elevation in the calyx[11] (100 nM). The supra-linear $Ca^{2+}$ cooperativity for exocytosis[4,5,47] might suggest a greater amount of spike-evoked release enhancement following presynaptic depolarization and $Ca^{2+}$ entry than we observed. However, asynchronous transmission can deplete the pool of release-ready vesicles, diminishing availability for phasic transmission[33,34]. The resulting short-term depression of release can develop concomitantly with facilitation, one effect masking the other[30,31]. In this way, the capacity for depolarization-evoked strengthening of transmission in MLIs is limited by the superimposition of $Ca^{2+}$-dependent depression mediated by vesicle pool depletion. Though IPSC amplitudes were unchanged by subthreshold depolarization in EGTA, it may be that release enhancement was merely balanced by depression rather than fully blocked. EGTA only partially diminished depolarization-induced $Ca^{2+}$ elevation suggesting that the $Ca^{2+}$-dependent effects on release persisted in this condition. The

expression of facilitation and depression will depend on the relative $Ca^{2+}$ sensitivity of each mechanism.

As implied in our burst-firing experiment, the capacity for release-strengthening by subthreshold depolarization may be strongly limited by depletion. Non-homogenous pools of vesicles may populate presynaptic sites at MLIs, as they do at the calyx of Held[48]. Subthreshold depolarization may help recruit more reluctant vesicles, distinguished by their relative $Ca^{2+}$ sensitivity and/or distance from VSCCs, to participate in release during subsequent action potential-evoked transmission. Bulk $Ca^{2+}$ elevation evoked by repetitive firing may also recruit these vesicles, depleting their availability and thereby decreasing the capacity for subthreshold depolarization induced enhancement of release. That is, multiplicative non-linear processes are competing for overlapping vesicle pools to determine the expression of short-term plasticity. We expect that any reduction in the vesicle pool(s), mediated by preceding sub- or suprathreshold activity, would diminish enhancement of release induced by subthreshold depolarization.

### Functional implications

Subthreshold depolarization-induced regulation of spike-evoked release is clearly important in a number of cell types, though the mechanisms underlying the regulation may vary across brain regions[1–3,13,18,35]. In MLIs, the phenomenon appears to be entirely dependent on axonal $Ca^{2+}$, as observed for other forms of release-strengthening[6]. In contrast, at hippocampal mossy fiber synapses, it may be that the $Ca^{2+}$-dependence is restricted to proximal portions of the axon, whereas at more distal sites other mechanisms of strengthening are involved[13], such as potassium channel inactivation[3,42]. One clear difference between these two cell types is axonal length, mossy fibers being much longer than MLI axons. Even in MLIs, the increases in axonal $Ca^{2+}$ are, on average, larger in proximal than in distal portions of the axon, as expected from cable properties[18]. However, there was no correlation between the depolarization-induced enhancement of release and distance between the somata of synaptically connected pairs ($r^2 = 0.06$, $P = 0.23$, n = 27), though this comparison is likely compromised by the inaccuracy of this measurement in predicting axonal length. The present results suggest that $Ca^{2+}$-dependent plasticity induced by somatic depolarization will affect the gain of most synapses in short axon cells and at least proximal synapses in other cell types. However, it is likely that depolarization-induced plasticity does not simply monotonically decay with distance from the soma given the amount of variance we observed in our $Ca^{2+}$ imaging and paired recording experiments. The control of transmitter release by subthreshold synaptic input that precedes action potential initiation adds a new dimension to synaptic signaling and requires consideration when analyzing information transfer across synapses.

## Methods

### Slice preparation

Parasagittal slices from cerebellar vermi were prepared from Sprague Dawley rats (PND 14–20) in accordance with OHSU IACUC-approved protocols. Rats, following isoflurane anesthesia, were decapitated and the cerebellum was isolated. Slices (250–300 μm) were cut

on a vibroslicer (Leica Instruments, Nussloch, Germany) in an ice-cold solution containing (in mM) 87 NaCl, 25 $NaHO_3$, 2.5 KCl, 1.25 $NaH_2PO_4$, 7 $MgCl_2$, 0.5 $CaCl_2$, 10 glucose, and 75 sucrose. Slices were subsequently transferred to a holding chamber containing (in mM) 119 NaCl, 26.2 $NaHO_3$, 2.5 KCl, 1 $NaH_2PO_4$, 2 $MgCl_2$, 1 $CaCl_2$, 11 glucose and maintained at 34°C for 30 min, thereafter, at 22–25°C until use. For whole-cell recording, slices were placed in a submersion chamber and superfused with the same solution (22–25°C) altered by elevating $CaCl_2$ to 1.5 and reducing $MgCl_2$ to 1.5 mM, except where noted. All solutions were oxygenated by pre- or continuous equilibration with carbogen gas (95% $O_2$, 5% $CO_2$).

## Electrophysiology

Whole-cell recordings were obtained from MLIs identified with gradient-contrast infrared video microscopy[49] based on their location within the molecular layer and distinct morphology[15]. Patch pipettes used for current-clamped MLIs contained a solution of (in mM) 128 K-gluconate, 2 KCl, 9 HEPES, 4 $MgCl_2$, 4 NaATP, and 0.5 NaGTP and 9 $K_4$-BAPTA. For paired recordings, perforated access[50] to the presynaptic MLI was achieved by including amphotericin B (300 μg/ml, previously aliquoted in DMSO). Alexa Fluor 488 hydrazide (30 μM; Molecular Probes; Eugene, OR) was also included in the pipette to fluorescently monitor the integrity of the perforated recording with light microscopy. If the patch membrane ruptured, resulting in cell fluorescence, recording was terminated. For $Ca^{2+}$ imaging experiments, $K_4$-BAPTA was replaced with 200μM Fluo-5F and 13μM Alexa Fluor 594 hydrazide (Molecular Probes, Eugene, OR). Current-clamped cells were held near −70 mV with constant current injection. Action potentials were stimulated between 0.3 to 0.1 Hz (~25–60 trials per condition). MLIs were voltage-clamped with a pipette solution containing (in mM) 135 CsCl, 10 HEPES, 4 $Mg_2ATP$, 0.3 NaGTP and 5 EGTA. The holding potential was kept at −60 mV giving rise to inward $GABA_AR$-mediated currents ($E_{Cl-} \approx 0$ mV). All pipettes had open-tip resistances of 3–12 MΩ.

Electrophysiological potentials and currents were recorded with a Multiclamp 700B amplifier (Molecular Devices, Union City, CA). Electrode series resistance was compensated by bridge balance in current-clamped cells and was uncompensated in the voltage-clamp configuration. Analog signals were filtered at 3–10 kHz and digitized at 20–50 kHz with a 16-bit A/D converter (Instrutech Corp., Port Washington, NY). High access resistance (40–80 MΩ) in the presynaptic perforated recording also likely contributed to filtering and action potential attenuation, though, access often improved during an experiment due to continued partitioning of the antibiotic. Data were collected using custom software (J.S. Diamond) written in IgorPro (Wavemetrics, Lake Oswego, OR) and analyzed using Axograph (Axograph Scientific, Sydney, Australia). $GABA_AR$-mediated synaptic responses were isolated with NBQX (10 μM) and *D*-AP5 (50 μM) (Tocris Cookson, Ellisville, MO) to block fast glutamate receptor-mediated responses. Picrotoxin (100 μM) was also included during imaging experiments to eliminate $GABA_AR$-mediated transmission. EGTA-AM (10–20 μM, Molecular Probes, Eugene, OR), made from a stock 100 mM solution in DMSO, was applied for at least 10 minutes during which data acquisition ceased. Upon resumption, EGTA-AM was continuously applied until the end of the experiment. In amplified views shown in figures, spontaneous IPSCs that were not time-locked to the presynaptic action potential were blanked prior to averaging for illustrative

purposes; events were only included within 1 ms after the action potential peak. In our analysis, however, spontaneous events were left unmodified.

### Two-photon laser-scanning microscopy

Fluorescence was monitored with a lab-built 2PLSM using an Olympus (Melville, NY) upright microscope, objective (60X, 1.0 NA), and oil-immersion condenser (1.4 NA). A Ti:sapphire laser (Coherent, Santa Clara, CA) tuned to 810 nm was used for excitation. Emitted green and red fluorescence were simultaneously collected by photomultiplier modules (H8224, Hamamatsu, Hamamatsu City, Japan) in both epi- and transfluorescence pathways using a 565 nm dichroic and 525/50 and 620/60 bandpass filters (Chroma, Battleboro, VT). Images were acquired using ScanImage software(K. Svoboda). Line scans were obtained at 500 Hz. Cells were filled for a minimum of 20 minutes prior to acquisition to allow for dye equilibration (axon varicosities <150 μm from the soma). For varicosities >150 μm from the soma, longer equilibration times were used.

Imaging analysis was performed offline using ImageJ (National Institutes of Health) and Axograph. Fluorescence changes were quantified as increases in green fluorescence normalized to red fluorescence ( G/R). Peak amplitude measurements of subthreshold depolarization-evoked $Ca^{2+}$ transients were determined by averaging a 100 ms epoch prior to action potential firing. Alternating trials in which no stimulation occurred were used to subtract background fluorescence levels; the difference reflecting the peak response. The peak of action potential-evoked $Ca^{2+}$ transients were determined from exponential fits of the fluorescence decay following stimulation (measured at t = 0). Changes in the peak amplitude of action potential-evoked responses might be underestimated if the indicator were in the non-linear range. The $Ca^{2+}$ transients evoked by subthreshold depolarization were usually very small. Therefore, for illustrative purposes only, we integrated these responses to accentuate the rise in $Ca^{2+}$ from the baseline noise during the subthreshold stimulus (Fig. 2b, 3a). This method was not included in any quantification.

### Statistical Analysis

Reported values are mean ± SEM. Excel (Microsoft) and InStat (GraphPad Software) were used for statistical analysis using paired and unpaired t-tests (two-tailed). ANOVA with post-hoc Tukey's tests were used when making multiple comparisons. Differences were considered statistical significance with α values of $P < 0.05$. In figures, asterisks denote statistical significance.

## Supplementary Material

Refer to Web version on PubMed Central for supplementary material.

## Acknowledgments

# References

1. Alle H, Geiger JRP. Combined analog and action potential coding in hippocampal mossy fibers. Science. 2006; 311:1290–1293. [PubMed: 16513983]

2. Shu Y, Hasenstaub A, Duque A, Yu Y, McCormick DA. Modulation of intracortical synaptic potentials by presynaptic somatic membrane potential. Nature. 2006; 441:761–765. [PubMed: 16625207]

3. Kole MHP, Letzkus JJ, Stuart GJ. Axon initial segment Kv1 channels control action potential waveform and synaptic efficacy. Neuron. 2007; 55:633–647. [PubMed: 17698015]

4. Bollmann JH, Sakmann B, Borst JGG. Calcium sensitivity of a glutamate release in a calyx-type terminal. Science. 2000; 289:953–957. [PubMed: 10937999]

5. Schneggenburger R, Neher E. Intracellular calcium dependence of transmitter release rates at a fast synapse. Nature. 2000; 406:889–893. [PubMed: 10972290]

6. Zucker RS, Regehr WG. Short-term synaptic plasticity. Ann Rev Physiol. 2002; 64:355–405. [PubMed: 11826273]

7. Sabatini BL, Regehr WG. Control of neurotransmitter release by presynaptic waveform at the granule to Purkinje cell synapse. J Neurosci. 1997; 17:3425–3435. [PubMed: 9133368]

8. Borst JGG, Sakmann B. Calcium influx and transmitter release in a fast CNS synapse. Nature. 1998; 383:431–434. [PubMed: 8837774]

9. Bischofberger J, Geiger JR, Jonas P. Timing and efficacy of $Ca^{2+}$ channel activation in hippocampal mossy fiber boutons. J Neurosci. 2002; 22:10593–105602. [PubMed: 12486151]

10. Brenowitz SD, Regehr WG. Reliability and heterogeneity of calcium signaling at single presynaptic boutons of cerebellar granule cells. J Neurosci. 2007; 27:7888–7898. [PubMed: 17652580]

11. Awatramani GB, Price GD, Trussell LO. Modulation of transmitter release by presynaptic resting potential and background calcium levels. Neuron. 2005; 48:109–121. [PubMed: 16202712]

12. Hori T, Takahashi T. Mechanisms underlying short-term modulation of transmitter release by presynaptic depolarization. J Physiol. 2009; 587:2987–3000. [PubMed: 19403620]

13. Scott R, Ruiz A, Henneberger C, Kullmann DM, Rusakov DA. Analog modulation of mossy fiber transmission is uncoupled from changes in presynaptic $Ca^{2+}$ J Neurosci. 2008; 28:7765–7773. [PubMed: 18667608]

14. Trigo FF, Bouhours B, Rostaing P, Papgeorgiou G, Corrie JET, Triller A, Ogden D, Marty A. Presynaptic miniature Gabaergic currents in developing interneurons. Neuron. 2010; 66:235–247. [PubMed: 20435000]

15. Palay, SL.; Chan-Palay, V. Cerebellar cortex: cytology and organization. Springer-Verlag; New York: 1974.

16. Mejia-Gervacio S, Collin T, Pouzat C, Tan YP, Llano I, Marty A. Axonal speeding: shaping synaptic potentials in small neurons by the axonal membrane compartment. Neuron. 2007; 53:843–855. [PubMed: 17359919]

17. Glitsch M, Marty A. Presynaptic effects of NMDA in cerebellar Purkinje cells and interneurons. J Neurosci. 1999; 19:511–519. [PubMed: 9880571]

18. Christie JM, Jahr CE. Dendritic NMDA receptors activate axonal calcium channels. Neuron. 2008; 60:298–307. [PubMed: 18957221]

19. Vincent P, Marty A. Fluctuations of inhibitory postsynaptic currents in Purkinje cells from rat cerebellar slices. J Physiol. 1996; 494:183–199. [PubMed: 8814615]

20. Diana MA, Marty A. Characterization of depolarization-induced suppression of inhibition using paired interneuron-Purkinje cell recordings. J Neurosci. 2003; 23:5906–5918. [PubMed: 12843295]

21. Llano I, Tan YP, Caputo C. Spatial heterogeneity of intracellular $Ca^{2+}$ signals in axons of basket cells from the rat cerebellar slices. J Physiol. 1997; 502:509–519. [PubMed: 9279804]

22. Forti L, Pouzat C, Llano I. Action potential-evoked $Ca^{2+}$ signals and calcium channels in the axons of developing cerebellar interneurons. J Physiol. 2000; 527:33–48. [PubMed: 10944168]

23. Tottene A, Moretti A, Pietrobon D. Functional diversity of P-type and R-type calcium channels in rat cerebellar neurons. J Neurosci. 1996; 16:6353–6363. [PubMed: 8815914]

24. Metz AE, Jarsky T, Martina M, Spruston N. R-type calcium channels contribute to afterdepolarization and bursting in hippocampal CA1 pyramidal neurons. J Neurosci. 2005; 25:5763–5773. [PubMed: 15958743]

25. Borst JGG, Sakmann B. Facilitation of presynaptic calcium currents in the rat brainstem. J Physiol. 1998; 513:149–155. [PubMed: 9782166]

26. Cuttle MF, Tsujimoto T, Forsythe ID, Takahashi T. Facilitation of the presynaptic calcium current at an auditory synapse in the rat brainstem. J Physiol. 1998; 512:723–729. [PubMed: 9769416]

27. Atluri PP, Regehr WG. Determinants of the time course of facilitation at the granule cell to Purkinje cell synapse. J Neurosci. 1996; 16:5661–5671. [PubMed: 8795622]

28. Bucurenciu I, Kulik A, Schwaller B, Frotscher M, Jonas P. Nanodomain coupling between $Ca^{2+}$ channels and $Ca^{2+}$ sensors promotes fast and efficient transmitter release at a cortical GABAergic synapse. Neuron. 2008; 57:536–545. [PubMed: 18304483]

29. Bucurenciu I, Bischofberger J, Jonas P. A small number of open $Ca^{2+}$ channels trigger transmitter release at a central GABAergic synapse. Nature Neurosci. 2010; 13:19–21. [PubMed: 20010820]

30. Dittman JS, Kreitzer AC, Regehr WG. Interplay between facilitation, depression, and residual calcium at three presynaptic terminals. J Neurosci. 2000; 20:1374–1385. [PubMed: 10662828]

31. Müller M, Goutman JD, Kochubey O, Schneggenburger R. Interaction between facilitation and depression at a large CNS synapse reveals mechanisms of short-term plasticity. J Neurosci. 2010; 30:2007–2016. [PubMed: 20147529]

32. Atluri PP, Regehr WG. Delayed release of neurotransmitter from cerebellar granule cells. J Neurosci. 1998; 18:8214–8227. [PubMed: 9763467]

33. Lu T, Trussell LO. Inhibitory transmission mediated by asynchronous transmitter release. Neuron. 2000; 26:683–694. [PubMed: 10896163]

34. Otsu Y, Shahrezaei V, Li B, Raymond LA, Delaney KR, Murphy TH. Competition between phasic and synchronous release for recovered synaptic vesicles at developing hippocampal autaptic synapses. J Neurosci. 2004; 24:420–433. [PubMed: 14724240]

35. Christie JM, Jahr CE. Selective expression of ligand-gated ion channels in L5 pyramidal cell axons. J Neurosci. 2009; 29:11450–11441.

36. Li L, Bischofberger J, Jonas P. Differential gating and recruitment of P/Q-, N-, and R-type $Ca^{2+}$ channels in hippocampal mossy fiber boutons. J Neurocsi. 2007; 27:13420–13429.

37. Wu LG, Borst JGG, Sakmann B. R-type $Ca^{2+}$ currents evoke transmitter release at a rat central synapse. Proc Natl Acad Sci USA. 1998; 95:4720–4725. [PubMed: 9539805]

38. Llano I, González J, Caputo C, Lai FA, Blayney LM, Tan YP, Marty A. Presynaptic calcium stores underlie large-amplitude miniature IPSCs and spontaneous calcium transients. Nature Neurosci. 2000; 12:1256–1265. [PubMed: 11100146]

39. Tsujimoto T, Jeromin A, Saitoh N, Roder JC, Takahashi T. Neural calcium sensor 1 and activity-dependent facilitation of P/Q-type calcium currents at presynaptic nerve terminals. Science. 2002; 295:2276–2279. [PubMed: 11910115]

40. Jinno S, Jeromin A, Roder J, Kosaka T. Immunocytochemical localization of neural calcium sensor-1 in the hippocampus and cerebellum of the mouse, with special reference to presynaptic terminals. Neurosci. 2002; 113:449–461.

41. Jinno S, Jeromin A, Kasaka T. Expression and possible role of neuronal calcium sensor-1 in the cerebellum. Cerebellum. 2004; 3:83–88. [PubMed: 15233574]

42. Geiger JRP, Jonas P. Dynamic control of presynaptic $Ca^{2+}$ inflow by fast-inactivating $K^+$ channels in hippocampal mossy fiber boutons. Neuron. 2000; 28:927–939. [PubMed: 11163277]

43. Turecek R, Trussell LO. Presynaptic glycine receptors enhance transmitter release at a mammalian central synapse. Nature. 2001; 411:587–590. [PubMed: 11385573]

44. Felmy F, Neher E, Schneggenburger R. Probing the intracellular calcium sensitivity of transmitter release during synaptic facilitation. Neuron. 2003; 37:801–811. [PubMed: 12628170]

45. Müller M, Felmy F, Schneggenburger R. A limited contribution of $Ca^{2+}$ current facilitation to paired-pulse facilitation of transmitter release at the rat calyx of Held. J Physiol. 2008; 586:5503–5520. [PubMed: 18832426]

46. Tang Y, Schlumpberger T, Kim T, Lueker M, Zucker RS. Effects of mobile buffers on facilitation: experimental and computational studies. Biophys J. 2000; 78:2735–2751. [PubMed: 10827959]

47. Heidelberger R, Heinemann C, Neher E, Matthews G. Calcium dependence of the rate of exocytosis in a synaptic terminal. Nature. 1994; 371:513–515. [PubMed: 7935764]

48. Wu L-G, Borst JGG. The reduced release probability of releasable vesicles during recovery from short-term synaptic depression. Neuron. 1999; 23:821–832. [PubMed: 10482247]

49. Dodt HU, Eder M, Schierloh A, Zieglgansberger W. Infrared-guided laser stimulation of neurons in brain slices. Sci STKE. 2002:PL2. [PubMed: 11854538]

50. Rae J, Cooper K, Gates P, Watsky M. Low access resistance perforated patch recordings using amphotericin B. J Neurosci Methods. 1991; 37:15–26. [PubMed: 2072734]
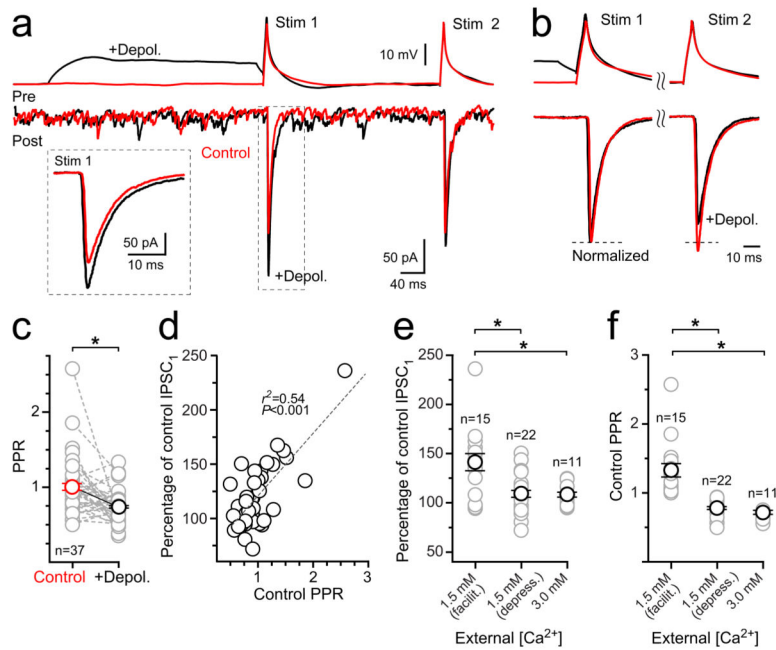
**Figure 1. Subthreshold somatic depolarization enhances spike-evoked release in MLIs**
(**a**) In a MLI paired recording, action potentials in the presynaptic neuron evoked $GABA_AR$-mediated IPSCs in the postsynaptic neuron. Subthreshold somatic depolarization (300 ms) elicited prior to spiking enhanced release. Control action potential responses are in red and test responses preceded by subthreshold depolarization are in black. An amplified view of the first IPSC is shown in the inset. (**b**) Paired-pulse IPSCs from the same neuron normalized to the peak of the first response. (**c**) Summary data show that the PPR decreases with somatic depolarization of the presynaptic neuron. A significant difference (paired t-test, $P < 0.05$) between groups is indicated by asterisk with mean values ± SEM. (**d**) Linear regression analysis indicates that release enhancement elicited by subthreshold depolarization was correlated with the basal PPR. (**e** and **f**) Differences in release enhancement for facilitating and depressing responses measured in 1.5 and 3.0 mM extracellular $Ca^{2+}$. ANOVA analysis with post-hoc Tukey's multiple comparison tests indicated significance ($P < 0.05$) with mean values plotted ± SEM. For clarity, spontaneous IPSCs were blanked prior to averaging in **a** (inset) and **b**.
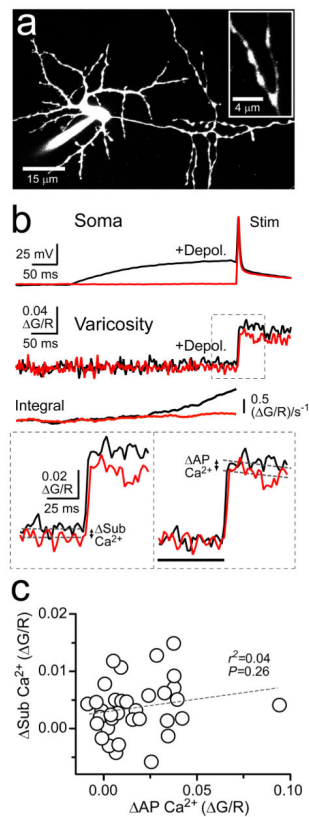
**Figure 2. Subthreshold somatic depolarization evokes and enhances axonal Ca$^{2+}$ entry**
(**a**) Two-photon fluorescence image of a representative MLI filled via patch pipette with Alexa 594 (13 μM) and Fluo-5F (200 μM). On the right, a higher-magnification view shows axon varicosities. (**b**) Somatic current injection elicited control action potential-evoked responses (red) and test spikes paired with 300 ms subthreshold depolarizations (black). Shown directly below are the resulting Ca$^{2+}$ transients recorded in an axon varicosity. Integration of the Ca$^{2+}$ signals accentuates the difference between control and depolarized responses prior to spike firing. At the bottom left, amplified view of Ca$^{2+}$ transients with dashed lines (100 ms epoch average) demarcating the amplitude of the Ca$^{2+}$ response evoked by subthreshold depolarization. On the bottom right, action potential-evoked Ca$^{2+}$ transients baselined prior to spike firing (black bar) isolated depolarization-dependent facilitation of the spike-evoked Ca$^{2+}$ transient. Exponential fits to the spike-elicited transients were used to determine peak amplitudes. (**c**) Comparison of depolarization-evoked Ca$^{2+}$ elevation and facilitation of action potential-elicited Ca$^{2+}$ entry. Line fit of the linear regression is indicated by the dashed line.
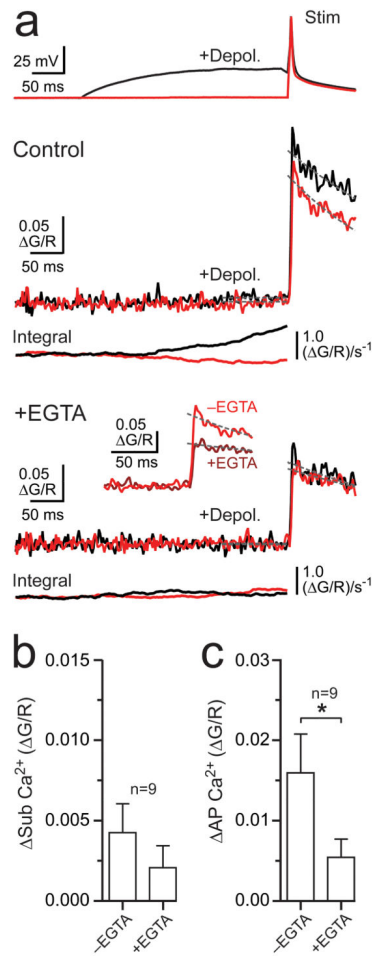
**Figure 3. Subthreshold depolarization-dependent Ca$^{2+}$ signaling is EGTA-sensitive**
(**a**) Somatic recording of an action potential (red) and an action potential preceded by a 300 ms subthreshold depolarization (black). The resulting Ca$^{2+}$ transients in an axon varicosity are shown below in control and following EGTA-AM application (10–20 μM; >10 min). Integrals of the Ca$^{2+}$ responses are provided for each condition. The inset shows a comparison of action potential-evoked responses, elicited without preceding subthreshold depolarization, in control and with EGTA. Dashed lines indicate the response amplitude prior to spiking (100 ms epoch) and the exponential fits of action potential-evoked Ca$^{2+}$ transients used to determine peak amplitudes. (**b**) The effect of EGTA on Ca$^{2+}$ entry evoked by subthreshold depolarization. (**c**) EGTA inhibits facilitation of spike-evoked Ca$^{2+}$ entry caused by subthreshold depolarization. Mean values are presented with error bars (+SEM); asterisks denote significance (paired t-test, $P < 0.05$).
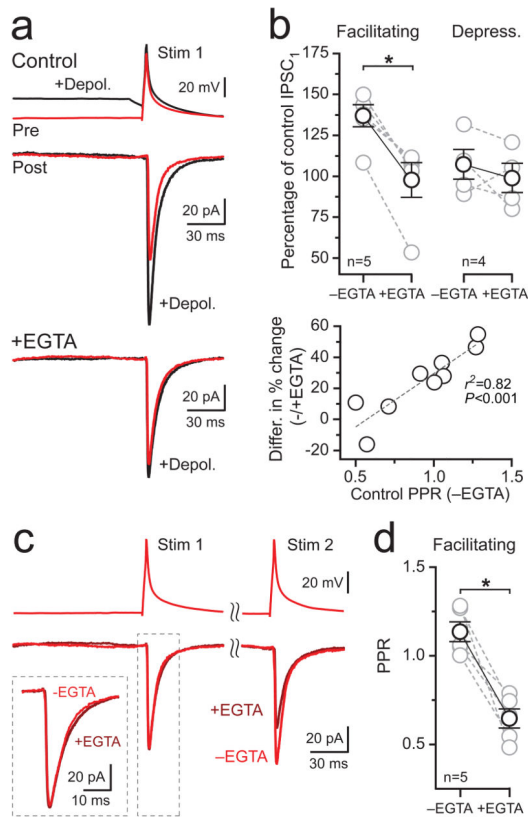
**Figure 4. EGTA inhibits enhancement of release elicited by subthreshold depolarization**
(**a**) Action potential-evoked IPSCs (red) recorded from pairs of connected MLIs in control and following EGTA-AM application. In alternating trials, action potentials were preceded by a 300 ms subthreshold depolarization (black). (**b**) Top summary graph shows that EGTA eliminates release strengthening caused by subthreshold depolarization in facilitating cell pairs. Release-strengthening was not apparent in cell pairs that depressed in basal conditions. In the bottom graph, linear regression analysis plots the difference between the percentage change in EGTA and in control relative to the basal PPR. (**c**) The effect of EGTA on paired-pulse responses from trials without preceding subthreshold depolarization. Amplified view of the first IPSC is shown on the inset. (**d**) EGTA altered paired-pulse responses in cell pairs that facilitated in basal conditions. Data are plotted as mean values with ± SEM and asterisks denote significance (paired t-test, $P < 0.05$). Spontaneous IPSCs were blanked prior to averaging in **a** and **c**.
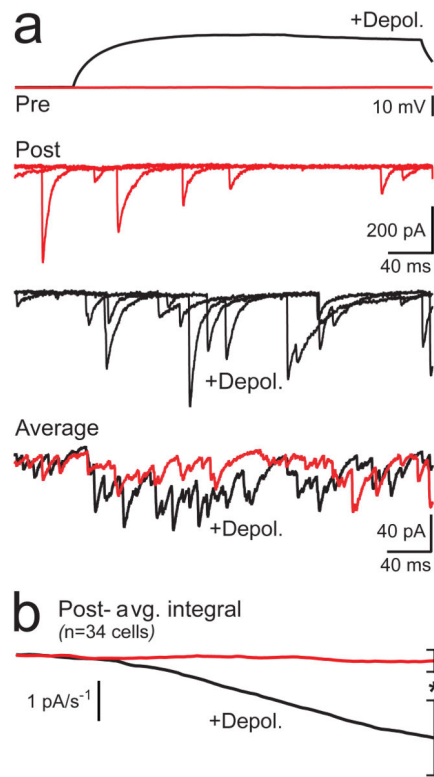
**Figure 5. Subthreshold depolarization evokes asynchronous release**
(**a**) Paired recording of MLIs show spontaneous IPSCs in unstimulated control responses
(red) and recruitment of asynchronous events with a 300 ms presynaptic subthreshold
depolarization (black). Three individual sweeps from the postsynaptic neuron are shown
superimposed for each condition with the average response (27 and 28 sweeps, control and
depolarized, respectively) at the bottom. (**b**) The average charge integration of the
postsynaptic response across all cell recordings (± SEM). Asterisk denotes significance
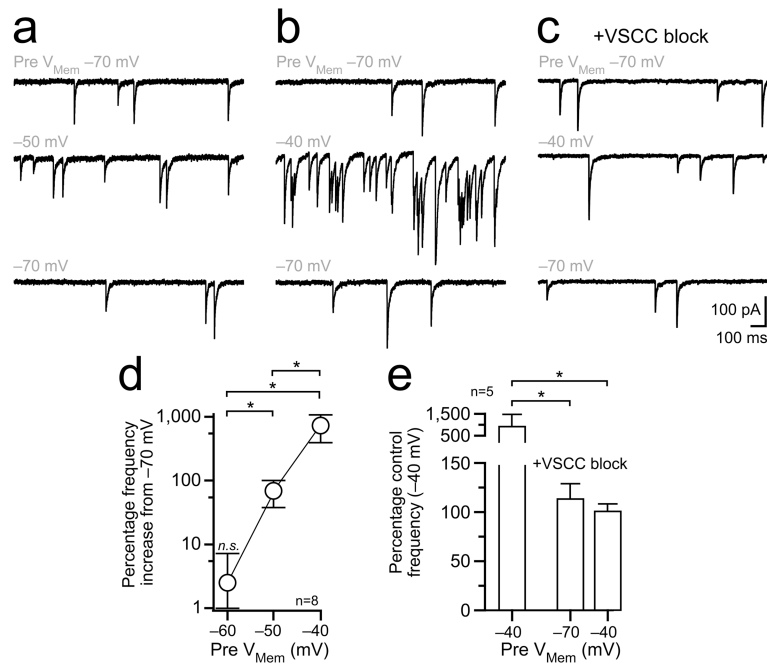(paired t-test, $P < 0.05$).

**Figure 6. Depolarization-dependent asynchronous release is triggered by VSCCs**
(**a,b**) Paired recording from MLIs in TTX with representative sweeps from the postsynaptic neuron showing recruitment of asynchronous IPSCs with presynaptic depolarization. The presynaptic holding potential is indicated in gray above each sweep. Responses were recorded in 3 mM extracellular $Ca^{2+}$ to enhance release. (**c**) In the same cell, IPSC frequency is unaltered by presynaptic depolarization after VSCC block (100 μM $Cd^{2+}$ and $Ni^{2+}$). (**d**) Asynchronous IPSC frequency depends on the presynaptic holding potential. Mean values are plotted with error bars ± SEM. Asterisks denote significant differences ($P < 0.05$) between groups tests following ANOVA analysis (Tukey's multiple comparison test). (**e**) Block of VSCCs eliminates the depolarization-dependent increase in asynchronous transmission. Mean values + SEM are shown with significance (asterisks $P < 0.05$) determined by ANOVA analysis.
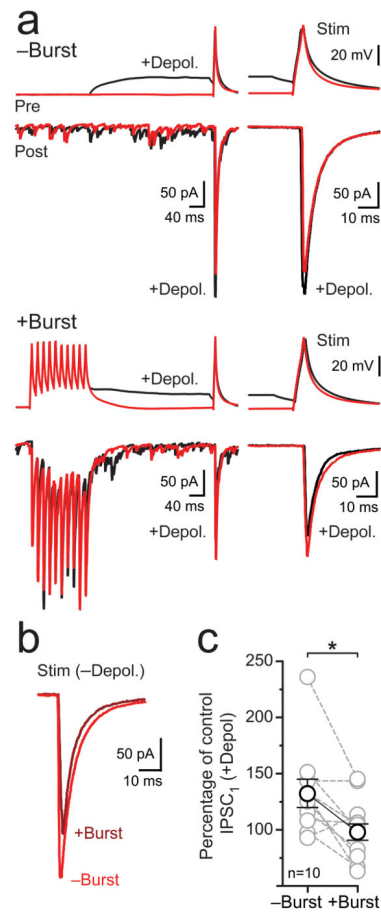
**Figure 7. Burst firing reduces the capacity for release enhancement caused by depolarization**
(**a**) In a recording from connected MLIs, high-frequency bursts of action potentials (10 spikes, 60 Hz) preceded a 300 ms subthreshold stimulation and test spikes in interleaved trials. Amplified views on the right show release enhancement caused by subthreshold depolarization and weakening of transmission when subthreshold excitation was paired with burst firing. (**b**) The effect of burst firing on the first IPSC in control trials without subthreshold stimulation is shown. (**c**) Burst firing eliminated release strengthening induced by subthreshold depolarization. Mean values are illustrated ± SEM with significance denoted by an asterisk (paired t-test, $P < 0.05$). For amplified views (**a** and **b**) spontaneous events were blanked prior to averaging.